INTERNATIONAL JOURNAL FOR NUMERICAL METHODS IN FLUIDS
Int. J. Numer. Meth. Fluids **29**: 501–514 (1999)

THE NUMERICAL SOLUTION OF THE TRANSIENT TWO-PHASE FLOW IN RIGID PIPELINES

EZZEDDINE HADJ-TAIEB[a] AND TAIEB LILI[b]

[a] *Department of Mechanics, Enis BPW, 3038 Sfax, Tunisia*
[b] *Department of Physics, Faculté des Sciences de Tunis, Tunis, Tunisia*

SUMMARY

Consideration is given in this paper to the numerical solution of the transient two-phase flow in rigid pipelines. The governing equations for such flows are two coupled, non-linear, hyperbolic, partial differential equations with pressure dependent coefficients. The fluid pressure and velocity are considered as two principle dependent variables. The fluid is a homogeneous gas–liquid mixture for which the density is defined by an expression averaging the two-component densities where a polytropic process of the gaseous phase is admitted. Instead of the void fraction, which varies with the pressure, the gas–fluid mass ratio (or the quality) is assumed to be constant, and is used in the mathematical formulation. The problem has been solved by the method of non-linear characteristics and the finite difference conservative scheme. To verify their validity, the computed results of the two numerical techniques are compared for different values of the quality, in the case where the liquid compressibility and the pipe wall elasticity are neglected. Copyright © 1999 John Wiley & Sons, Ltd.

KEY WORDS: characteristics method; finite differences scheme; transient flow; two-phase flow

1. INTRODUCTION

Two-phase flows occur in piping systems in several industries, such as nuclear and geothermal power plants, petroleum industries and sewage pipelines. The transient flow in these cases affects a mixture of different states, liquid and gaseous. As the gas–liquid mixture is compressible, the wave propagation velocity varies with the pressure [1] and the system of equations describing the transient two-phase flow is non-linear. Analytical solution of these equations is generally not available. Numerical solutions of the non-linear partial differential equations governing homogeneous two-phase transient flow have been treated by several authors during the last 30 years. These numerical solutions are more complex and difficult than those where the transient flow concerns pure liquid. The complexity arises when the wave front is computed as the expansion waves spread, the compression waves steepen and the shock wave inception may manifest.

Martin *et al.* [2] have developed two numerical methods: the method of characteristics and the finite difference Lax–Wendroff method. The finite difference method has been employed and preferred over the method of characteristics due to available facilities. Chaudry *et al.* [3], have used two second-order explicit finite-difference techniques coupled with the characteristic equations at the pipe boundaries. To develop the numerical solution of gaseous-cavitating transient flow, Wiggert and Sundquist [4] have utilized the method of characteristics based on the specified distance and time increments. However, this technique requires spatial interpolations resulting in some numerical dissipation of the pressure wave fronts.

CCC 0271–2091/99/050501–14$17.50

Most of the above mentioned investigations has modelled the homogeneous two-phase transient flow by using the void fraction which varies with the pressure.

The purpose of the present paper is to numerically investigate the non-linear behaviour of the transient two-phase flow. Instead of the void fraction, the developed model uses the gas–fluid mass ratio, or the quality as called by Pascal [5], assumed to be constant. The pipe elasticity and the liquid compressibility are neglected against the gas deformability. Since the governing equations of such flow are non-linear, the solution of the mathematical equations system can be obtained only by some approximate numerical techniques. Two numerical techniques are employed in this paper. They are the method of characteristics grid and the finite differences conservative method. Numerical results obtained by these two methods are compared for different values of the quality.

2. MATHEMATICAL MODEL

A one-dimensional mathematical model which describes the transient behaviour of gas–liquid mixture flow is presented. The model is based on conventional waterhammer theory. In this study, the liquid compressibility and the pipe wall elasticity are neglected relative to the gas deformability. The pipe conveying fluid at pressure p, is assumed to be cylindrical (of circular cross section) and has a constant diameter D. The mixture is assumed to be made of small gas bubbles uniformly distributed in the liquid and the slip velocity of gas bubbles relative to the liquid velocity is neglected. So the number of bubbles per unit fluid volume may be assumed to be constant and then the quality, or the gas–fluid mass ratio, may also be considered as constant. The wall shear stress is assumed to be the same as if the flow were steady and is defined by the steady state Darcy–Weisbach formula depending on the friction factor.

2.1. Two-phase mixture density

The two-phase homogeneous fluid is made of incompressible liquid containing gas bubbles uniformly distributed and evolving according to the polytropic process:

$$p/\rho_g^n = p_0/\rho_{g_0}^n, \tag{1}$$

where p is the pressure, ρ_g the gas density and n the polytropic exponent. The subscript 0 refers to the initial thermodynamics conditions.

By noting $\theta = M_g/(M_g + M_l)$, the gas–fluid mass ratio or the quality, the two-phase mixture density ρ may be expressed in terms of the two components densities as follows:

$$1/\rho = \theta/\rho_g + (1-\theta)/\rho_l. \tag{2}$$

Using relation (1), Equation (2) becomes:

$$\rho(p) = [(\theta/\rho_{g_0})(p_0/p)^{1/n} + (1-\theta)/\rho_l]^{-1}, \tag{3}$$

where ρ_l is the liquid density, assumed to be constant.

2.2. Motion equations

The equations which describe transient one-dimensional flow can be adapted from the analytical model developed by Streeter and Wylie [6]. Applying the law of conservation of mass and momentum, to an element of fluid between two sections x and $x + \mathrm{d}x$ of the pipe, yields the following equations of continuity and motion:

$$\partial\rho/\partial t + \partial(\rho V)/\partial x = 0 \tag{4}$$

$$\partial V/\partial t + V\,\partial V/\partial x + 1/\rho\ \partial p/\partial x = gI - \lambda V|V|/2D, \tag{5}$$

where V is the fluid velocity, I the slope of the pipe, λ is the coefficient of friction, A is the cross section area of the pipe, t is the time and x is the distance along the pipe.

3. NUMERICAL SOLUTION

The numerical solution of the initial boundary value problem governed by Equations (4) and (5) is described. Two numerical solution techniques are used. The method of characteristics has been discussed in detail by Abbott [7] and it has been used to solve various wave propagation problems in fluid by several authors, e.g. Streeter and Wylie [6], Wiggert and Sundquist [4], Wiggert and Stuckenbruck [8], Rachid and Stuckenbruck [9] and Tijsselling [10]. The method of characteristics, which is based on the propagation celerity of the pressure waves, is applied to obtain ordinary differential equations. In principle, it is not a numerical but an analytical solution method. However, some of the necessary integration is generally done numerically. The finite difference conservative method, for solving partial differential equations, is quite classical and the work of Lax–Wendroff [11], is an excellent reference for difference method for non-linear hyperbolic equations.

3.1. Method of characteristics

By introducing the wave speed C defined by:

$$C = (\partial\rho/\partial p)^{-1/2} = (\theta n p_0/\rho_{g_0})^{1/2}(p/p_0)^{(n-1)/2n}[1 + ((1-\theta)/\theta)(\rho_{g_0}/\rho_1)(p/p_0)^{1/n}] \tag{6}$$

and represented in Figure 1, the continuity equation may be rewritten as follows:

$$\frac{1}{\rho C^2}\left(\frac{\partial p}{\partial t} + V\frac{\partial p}{\partial x}\right) + \frac{\partial V}{\partial x} = 0. \tag{7}$$

Figure 1 indicates that the wave speed varies considerably with both the pressure and the quality. The other data from Equation (6) used in producing Figure 1 are:

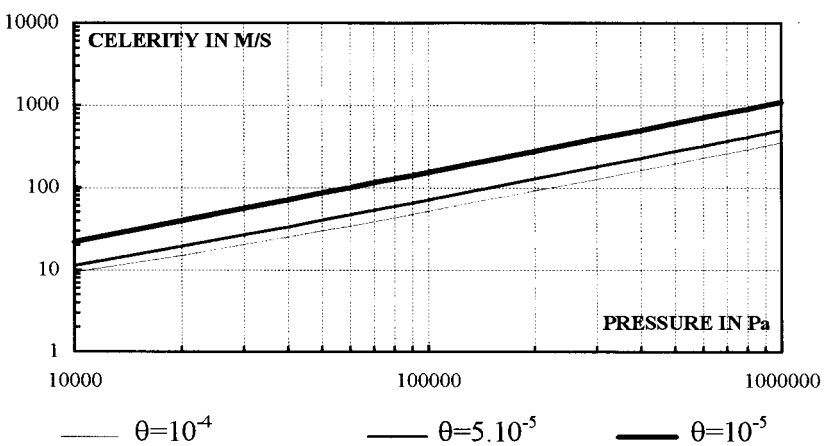

Figure 1. Pressure wave speed in rigid pipes.

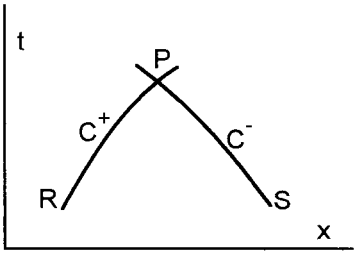

Figure 2. The characteristic lines in the x, t plane.

$$n = 1.4, \quad \rho_1 = 1000 \text{ kg m}^{-3}, \quad \rho_{g_0} = 1.29 \text{ kg m}^{-3}, \quad p_0 = 10^5 \text{ Pa}$$

By applying the characteristics theory [6], the following ordinary differential equations result:

$$C^+ \begin{cases} \mathrm{d}V + \mathrm{d}U = [gI - \lambda V|V|/(2D)]\,\mathrm{d}t \\ \mathrm{d}x = (V + C)\,\mathrm{d}t \end{cases} \tag{8}$$

and

$$C^- \begin{cases} \mathrm{d}V - \mathrm{d}U = [gI - \lambda V|V|/(2D)]\,\mathrm{d}t \\ \mathrm{d}x = (V - C)\,\mathrm{d}t \end{cases} \tag{9}$$

in which U is the Riemann invariant defined by:

$$\mathrm{d}U = \mathrm{d}p/(\rho C). \tag{10}$$

Taking Equations (3) and (6) into account, Equation (10) yields:

$$U = [2/(n-1)](n\theta p_0/\rho_{g_0})^{1/2}(p/p_0)^{(n-1)/2} \quad \text{and} \quad p = p_0\{[(n-1)/2][\rho_{g_0}/(n\theta p_0)]^{1/2}U\}^{2n/(n-1)}. \tag{11}$$

Thus the unknown values of V and U at any point P as shown in Figure 2, can be determined by finding their values at the points R and S lying on the two characteristics C^+ and C^- passing through P, and by integrating Equations (8) and (9) along the relevant characteristic lines.

The characteristics are curved lines on the x, t plane, so this integration can be achieved by means of an iterative trapezoidal integration rule [14]. We obtain the unknown values x_P, t_P, V_P, U_P:

$$t_P^k = \frac{1}{2}\frac{x_S - x_R + 1/2[(V_P + C_P)^{k-1} + (V_R + C_R)]t_R - 1/2[(V_P - C_P)^{k-1} + (V_S - C_S)]t_S}{1/2[(V_P + C_P)^{k-1} + (V_R + C_R)] + 1/2[(V_P - C_P)^{k-1} + (V_S - C_S)]} \tag{12}$$

$$x_P^k = x_R + \frac{1}{2}[(V_P + C_P)^{k-1} + (V_R + C_R)](t_P^k - t_R) \tag{13}$$

$$V_P^k = \frac{g}{4}\left\{[(I-J)_R + (I-J)_P^{k-1}](t_P^k - t_R) - [(I-J)_S + (I-J)_P^{k-1}](t_P^k - t_S) + \frac{V_R + U_R + V_S - U_S}{g/2}\right\} \tag{14}$$

$$U_P^k = U_R + V_R - V_P^k + \frac{g}{2}[(I-J)_R + (I-J)_P^{k-1}](t_P^k - t_R) \tag{15}$$

$J = -\lambda V|V|/(2Dg)$ is the head loss.

A grid of characteristics is now established in order to accomplish an orderly computer solution. The pipe of length L is initially discretized into N equal reaches, $\Delta x = L/N$. Hydraulic conditions are known along the pipe at the initial time (given by initial steady state conditions). Then through the use of Equations (12)–(15), we can find conditions at 1, 2 and 3 (Figure 3). With values of x, t, V, U known at each of these locations the grid can be continued to 4 and 5.

From the numerical solution developed in Reference [6], the above procedure must be slightly modified at the pipe boundaries by introducing the appropriate boundary conditions, specifying V_P and U_P or a relation between them in each case. The boundary conditions considered here are:

$$V(0, t) = 0 \text{ at the upstream end, and } U(L, t) = Cte = U_L \text{ at the downstream end.} \tag{16}$$

For relatively low values of the quality, shock waves will form and will be transmitted along the pipe. In this situation the characteristic grid tends to form an envelop when the shock wave is formed (see point Q in Figure 3). The solution cannot be extended beyond this point unless internal boundary conditions at the shock are included. For this reason, Martin *et al.* [2] preferred the finite differences scheme over the characteristics method. In this study we have deduced these conditions directly from the characteristics Equations (8) and (9). Also the iteration number is limited to $k = 5$.

3.2. Finite difference conservative method

The continuity equation (4) is in the so-called conservative form. Using the fluid density expression (3), the equation of motion (5) can also be formulated in this form, that is:

$$\frac{\partial V}{\partial t} + \frac{\partial}{\partial x}\left\{\frac{V^2}{2} + \left[\frac{n}{n-1}\frac{\theta}{\rho_{g_0}}\left(\frac{p_0}{p}\right)^{1/n} - \frac{(1-\theta)}{\rho_1}\right]p\right\} = gI - \frac{\lambda}{2D}V|V|. \tag{17}$$

Written in a conservation form, the system of continuity and motion (Equations (4) and (17)) can be solved with the two-step finite difference S_β^α scheme.

Following the techniques described by Lerat and Peyret [12], the two-step S_β^α scheme used on conservative Equations (4) and (17) for any grid point $(i, k+1)$, are as follows

First step of prediction (instant $(k+\alpha)\Delta t$)

$$\rho_{i+\beta}^{k+\alpha} = (1-\beta)\rho_i^k + \beta\rho_{i+1}^k - \alpha\sigma[(\rho V)_{i+1}^k - (\rho V)_i^k]$$

$$(V)_{i+\beta}^{k+\alpha} = (1-\beta)(V)_i^k + \beta(V)_{i+1}^k - \alpha\sigma[F_{i+1}^k - F_i^k] + \frac{g\Delta t}{2}[(I-J)_{i+1}^k + (I-J)_i^k]. \tag{18}$$

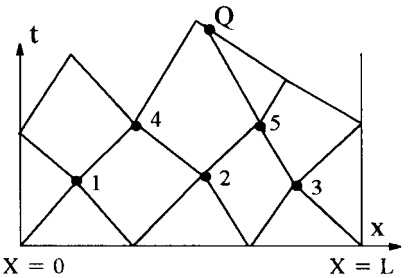

Figure 3. Characteristics grid.

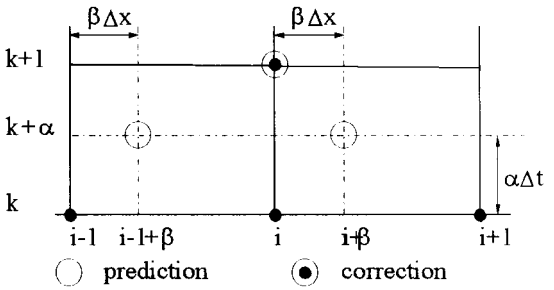

Figure 4. Finite differences scheme.

Second step of correction (instant $(k+1)\Delta t$)

$$\rho_i^{k+1} = \rho_i^k - \frac{\sigma}{2\alpha}\left[(\alpha-\beta)(\rho V)_{i+1}^k + (2\beta-1)(\rho V)_i^k + (1-\alpha-\beta)(\rho V)_{i-1}^k + (\rho V)_{i+\beta}^{k+\alpha} - (\rho V)_{i+\beta-1}^{k+\alpha}\right]$$

$$V_i^{k+1} = V_i^k - \frac{\sigma}{2\alpha}\left[(\alpha-\beta)F_{i+1}^k + (2\beta-1)F_i^k + (1-\alpha-\beta)F_{i-1}^k + F_{i+\beta}^{k+\alpha} - F_{i+\beta-1}^{k+\alpha}\right] + g\Delta t(I-J)_i^k, \tag{19}$$

where

$$F(p, V) = V^2/2 + \left[\frac{n}{n-1}(\theta/\rho_{g_0})(p_0/p)^{1/n} - (1-\theta)/\rho_1\right]p, \quad i = 1, \ldots, N+1$$

refer to grid points in the x-direction and k and $k+1$ refer to old and new time steps in the t-direction (Figure 4).

In these equations, $\sigma = \Delta t/\Delta x$ is the grid-mesh ratio and α, β are two parameters of values, generally satisfying the conditions $0 \le \alpha,\ \beta \le 1$. Note that the particular values $\alpha = 1/2$ and $\beta = 1/2$ correspond to the two-step Lax–Wendroff method [13]. The S_β^z scheme is a three-point, accurate method. It can be shown that the requirement condition for stability is given by the Courant–Friedrichs–Lewy condition:

$$\sigma \le 1/(|V| + C). \tag{20}$$

The finite difference equations (18) and (19) of the numerical scheme described herein, give the value of the velocity, V_i^{k+1}, directly. The Newton–Raphson method [14], is used to compute the pressure p_i^{k+1} from the calculated value of ρ_i^{k+1}:

$$\rho(p_i^{k+1}) - \rho_i^{k+1} = 0 \Rightarrow (p_i^{k+1})_{m+1} = (p_i^{k+1})_m - \{\rho[(p_i^{k+1})_m] - \rho_i^{k+1}\} \Big/ \left\{\frac{\partial\rho}{\partial p}[(p_i^{k+1})_m]\right\}. \tag{21}$$

Using Equation (6), the following iterative algorithm is obtained:

$$\begin{cases}(p_i^{k+1})_0 = p_i^k \\ (p_i^{k+1})_{m+1} = (p_i^{k+1})_m - C^2[(p_i^{k+1})_m]\{\rho[(p_i^{k+1})_m] - \rho_i^{k+1}\}\end{cases} \tag{22}$$

which indicates that the pressure wave speed interferes not only with the stability condition (20) but also with the finite difference scheme. m is the iteration number in the Newton–Raphson method.

The values of the hydraulic parameters at the time corresponding to $k = 0$, are given by the initial steady state conditions.

4. NUMERICAL RESULTS

Consider the hypothetical hydraulic system shown by Figure 5. The pipeline is horizontal $I = 0$, of length $L = 20\,000$ m and diameter $D = 2$ m. The fluid properties are:

$$\rho_l = 1000 \text{ kg m}^{-3}, \quad p_0 = 10^5 \text{ Pa}, \quad \rho_{g_0} = 1.29 \text{ kg m}^{-3}, \quad n = 1.4.$$

The head pressure at the pump is $H_0 = 100$ m, the initial flow rate is $Q_0 = 7.30 \text{ m}^3 \text{ s}^{-1}$ and the friction factor is $\lambda = 0.025$

4.1. Initial conditions

The initial conditions $(p_0(x), V_0(x))$ can be determined by computing the solution of the following system of ordinary differential equations:

$$\mathrm{d}(\rho V)/\mathrm{d}x = 0 \quad \text{and} \quad \mathrm{d}F(p, V)/\mathrm{d}x = g(I - J) \tag{23}$$

with the values for $x = 0$:

$$p_0(0) = \rho[p_0(0)]gH_0 + p_0 \quad \text{and} \quad V_0(0) = 4Q_0/(\pi D^2). \tag{24}$$

$\rho[p_0(0)]$ is computed from Equation (3) by the iterative method: $\rho_{m+1} = \rho(\rho_m g H_0 + p_0)$.

The desired solution of the differential equation (23) may be obtained by the Runge–Kutta algorithm [14]. The results are presented in Figure 6 for $\theta = 10^{-4}$.

4.2. Boundary conditions

Transient flow is created by a rapid pump failure at the upstream end $x = 0$, that is: $V(0, t) = 0$. At the downstream end, $x = L$ and $t > 0$, the condition is given by the reservoir at fixed level: $p(L, t) = p_0(L)$.

The pipe is divided into N equidistant sections in the x-direction $\Delta x = L/N$. From the CFL stability condition (23), the time increment Δt may be valued at:

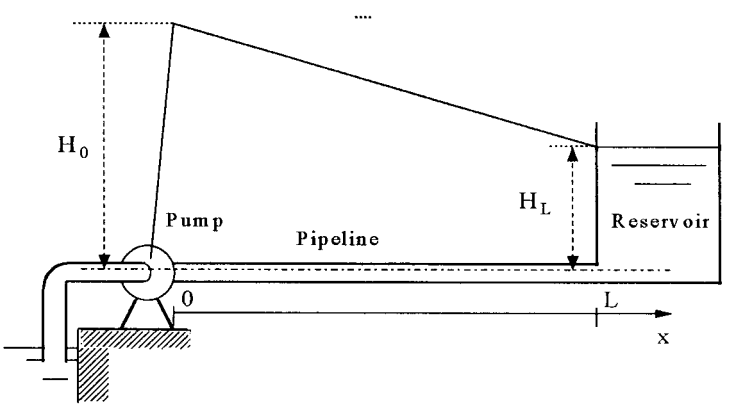

Figure 5. Hydraulic system.

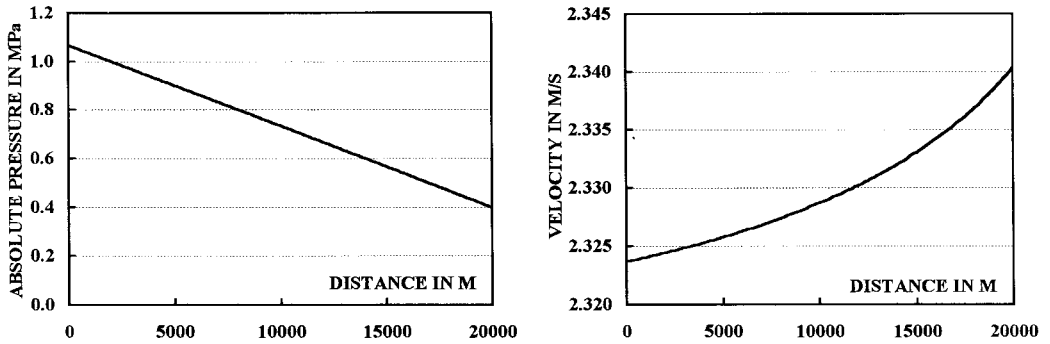

Figure 6. Initial steady state conditions.

$$\Delta t = L/[N^*(V_0(0) + C(p_0(0)))] \tag{25}$$

Two separate TURBO PASCAL programs were run on a HP 486/100 MHz computer. The same problem has been solved with both methods using 30 grid points for the method of characteristics and 120 grid points for the finite difference method. All the curves and the characteristics diagrams presented herein have been plotted using Microsoft Excel 5.0.

The computed pressure results of the method of characteristics and finite difference scheme S_0^1, obtained for the quality values $\theta = 10^{-4}$, $\theta = 5 \times 10^{-5}$, $\theta = 2.5 \times 10^{-5}$ and $\theta = 10^{-5}$, are shown in Figures 7 and 8. These pressures are at the upstream end ($x = 0$) and the middle ($x = L/2$) of the pipe. The agreement between these two methods is consistent, particularly for the large values of the quality.

The computed times required by these two methods to complete the solution to ≈ 1000 s are given together with the S_0^1 time step in Table I. It is clear that the characteristics method is less expensive than the finite differences scheme. Strelkoff [15] noted that explicit numerical schemes, such as the S_α^β method, require small steps in time because of stability. Moreover, as seen in Figure 9, with a comparatively small number of grid points ($N = 30$), the finite difference method results in too many oscillations and does not give smooth results.

Figures 7 and 8 illustrate the phenomenon we are dealing with in the case of rigid pipe and incompressible liquid. After the sudden pump failure, a negative pressure wave travels along the steady state pressure gradient until it reaches the downstream end of the pipe. A region of depression is developed for some time depending on the value of θ. The positive reflected pressure wave travelling from the end of the pipe causes pressure to rise. As the

Table I. The programs computed times

Quality (θ)	Characteristics method $N = 30$ and $k = 5$ (T)	Finite differences method (ΔT (T))		
		$N = 30$	$N = 60$	$N = 120$
10^{-4}	10″	2.026″ (6″)	1.013′ (15″)	0.55″ (50″)
5×10^{-5}	12″	1.435″ (8″)	0.718″ (20″)	0.359″ (70″)
2.5×10^{-5}	16″	1.016″ (10″)	0.508″ (29″)	0.254″ (100″)
10^{-5}	24″	0.549″ (16″)	0.274″ (48″)	0.137″ (180″)

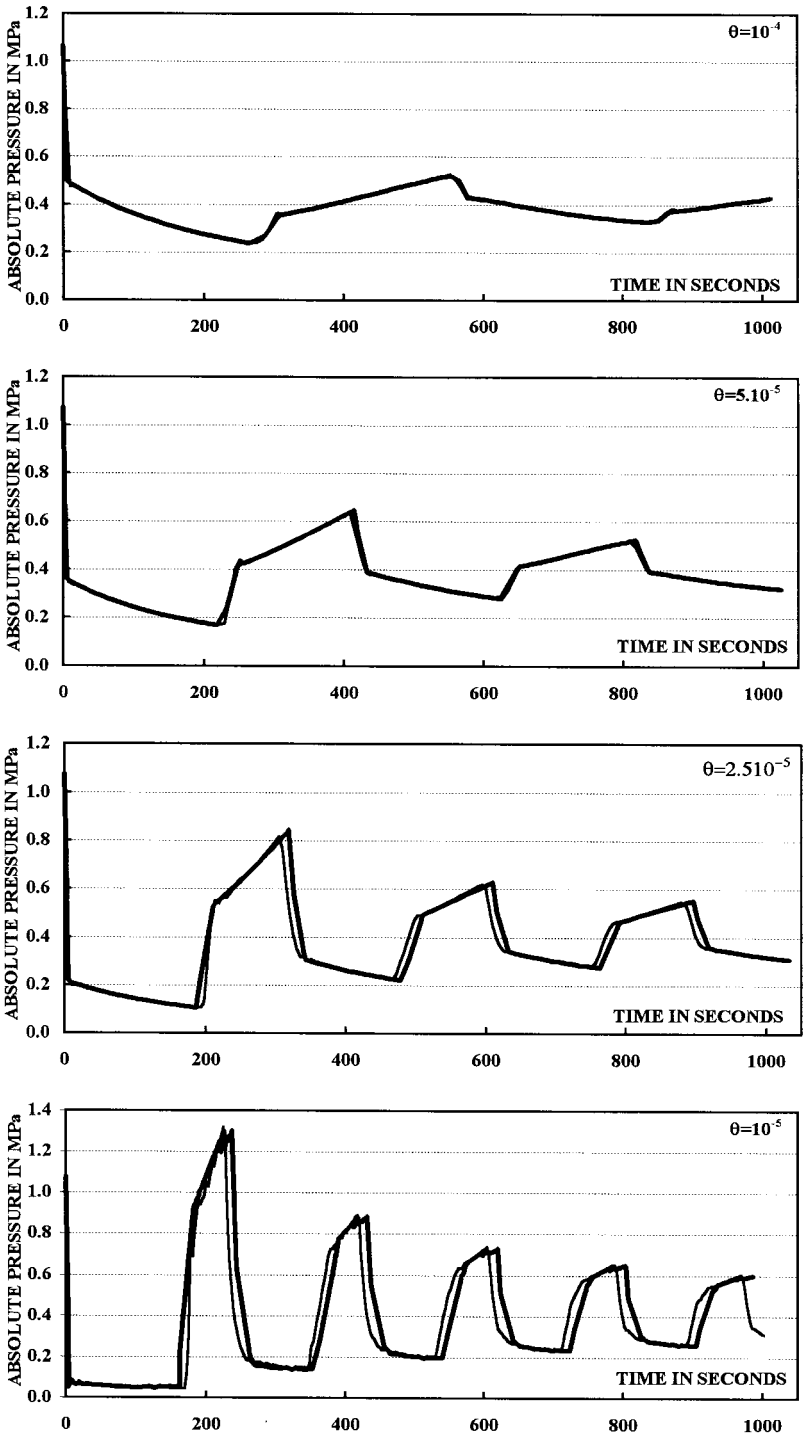

Figure 7. Calculated pressures at the upstream end of the pipe ($x = 0$). (Thin line) Finite differences S_0^1 scheme. (Thick line) Characteristics method.

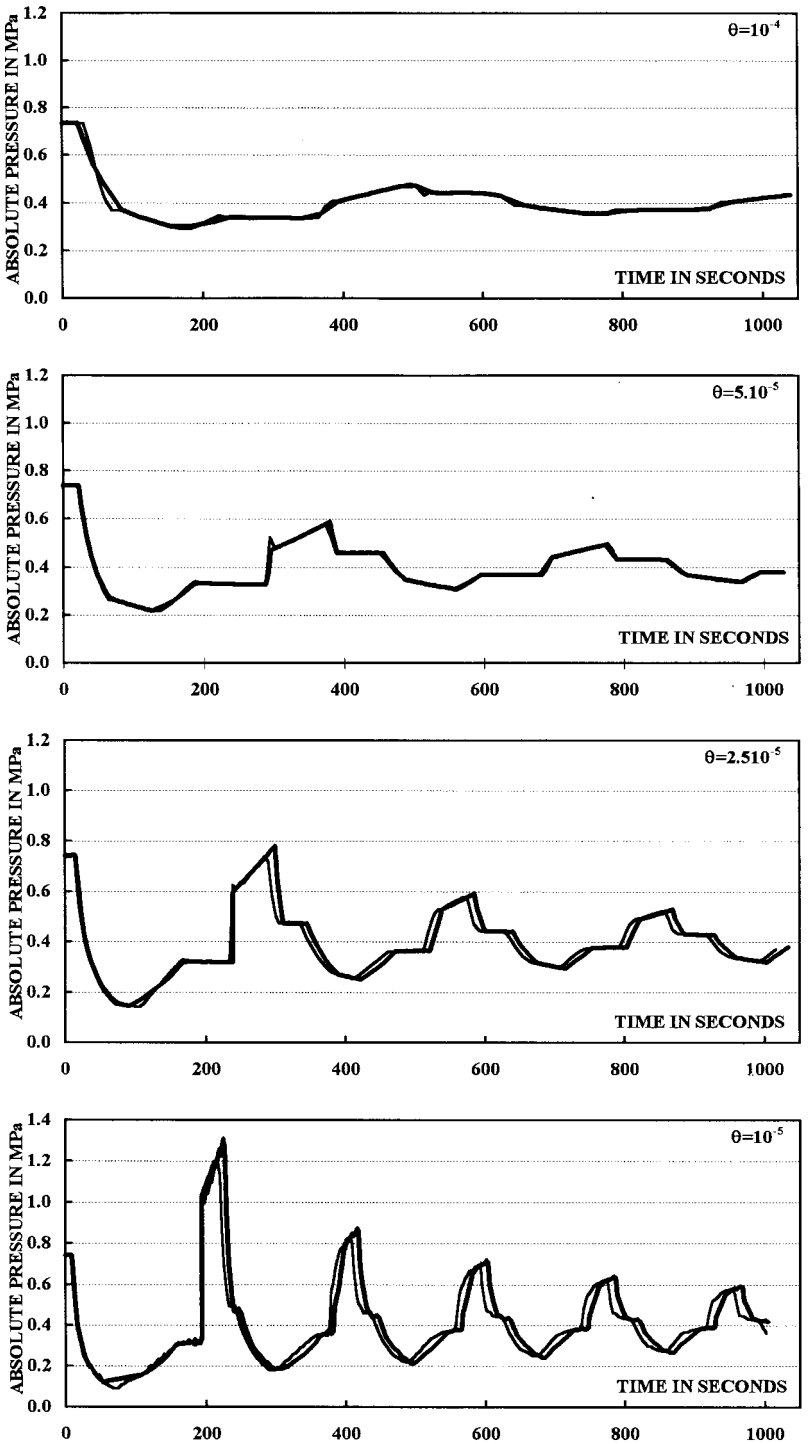

Figure 8. Calculated pressures at the middle of the pipe ($x = L/2$). (Thin line) Finite differences S_0^1 scheme. (Thick line) Characteristics method.

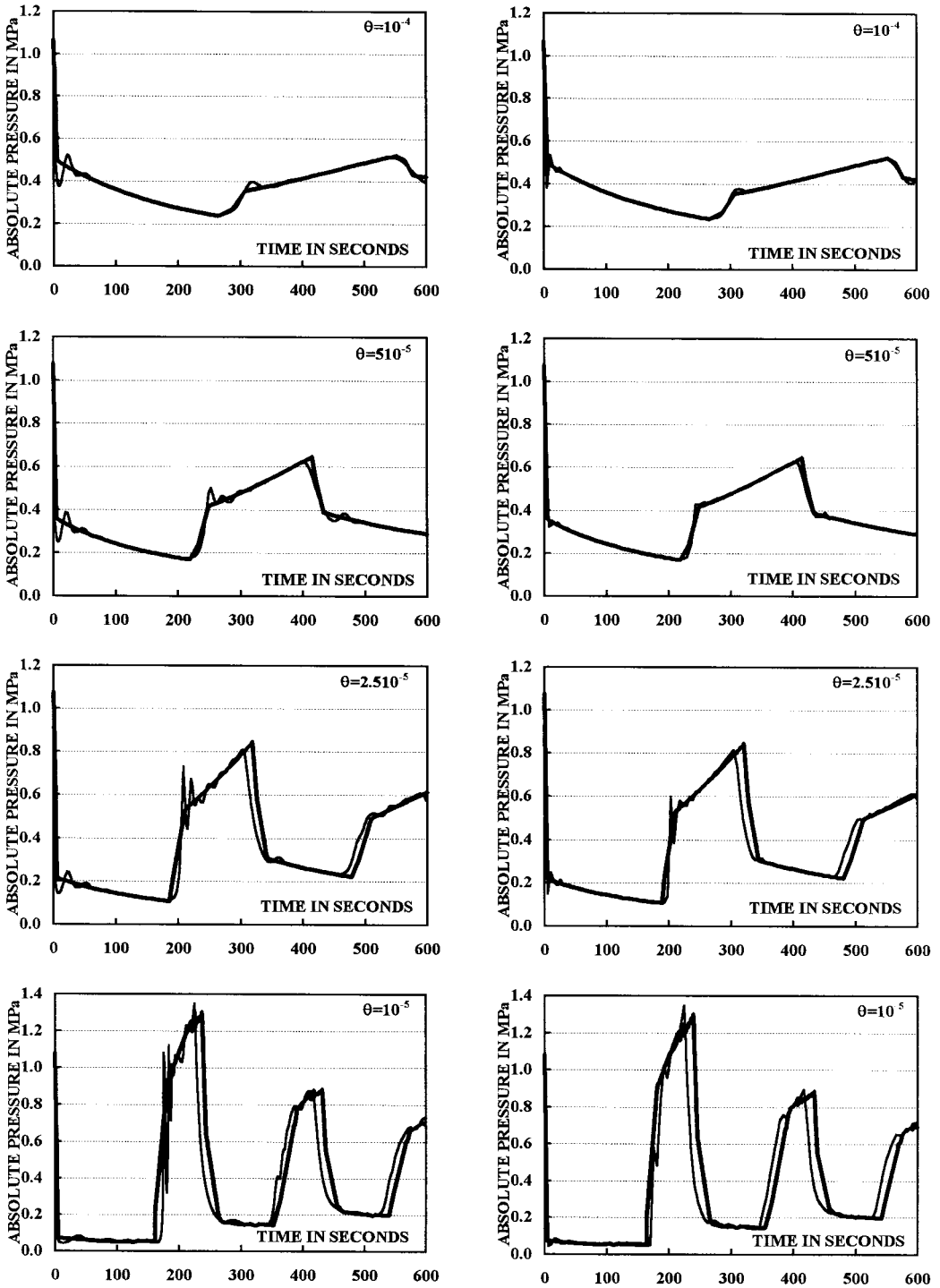

Figure 9. Calculated pressures at the upstream end of the pipe ($x = 0$). (Thin line) Finite difference S_0^1 scheme, on the left $N = 30$ and on the right side $N = 60$. (Thick line) Characteristics method.

waves are damped by wall friction, the overpressure does not exceed the downstream reservoir pressure (see Figure 8). The positive pressure propagates to the closed upstream end and reflects here, causing more overpressure. The process is repeated until the pressure fluctuations are dumped at the final steady state pressure.

It is possible to see that the presence of a great quantity of free gas ($\theta = 10^{-4}$) smoothes the reflected suppressions. This can be explained by the fact that for large values of θ, the fluid mixture becomes more compressible, which increases its capacity to attenuate the pressure fluctuations. For relatively small values of the quality, the overpressures become severe and provoke shock waves to occur.

Figure 10 shows the characteristic grids for the sudden shut-off of all flow at the upstream end of the pipe when the downstream pressure is maintained constant. Providing the final steady state has not been established, the behaviour of characteristic paths in the compression region differs from those of the depression region. For the relatively low values of the quality $\theta = 2.5 \times 10^{-5}$ and $\theta = 10^{-5}$, running together the grid lines indicates the existence of shocks which are transmitted along the pipe. In this case internal boundary conditions have been employed in the characteristics method. The phenomena of wave front spreading, wave front steepening and wave shock inception are well represented in the different characteristics diagrams. As the Excel 5.0 graphics logical capacity is limited to 4000 points, the characteristics lines are interrupted before reaching a time of 1000 s. By correctly reducing the value of N it is possible to represent the characteristic diagrams to this time.

5. SUMMARY AND CONCLUSION

The numerical solution of the transient two-phase flows in rigid pipelines has been presented in this paper. This problem is governed by two coupled non-linear partial differential equations of the hyperbolic type. The two numerical methods employed are the method of curved characteristics and the finite difference conservative method.

Of the two methods employed, the former seems to be the superior one. There is less computer cost involved with this method. Supplementary equations are, however, necessary in computing the hydraulic magnitudes at the shock wave front. The characteristics method allows visibility of the shock inception in the x, t plane, but it requires the use of the interpolation method to compute the pressure evolution at any interior section of the pipe. Nevertheless, these interpolations have no effects on the precision of the numerical solution and the evolution of the characteristic line.

The finite difference S_{β}^{α} method is more practical and correctly simulates the pressure wave propagation. The values of the hydraulic parameters at the pipe boundaries were simulated in this method without using characteristic equations, but they were deduced directly from the numerical scheme equations presented herein. The minor oscillations appearing in the pressure curves may be reduced by choosing the time increment at the limit of the stability condition and by increasing the number of the grid points. This method captures the shock wave with precision, without any special treatment, and the pressure–time curves are easily determined at any section of the pipe. The Newton–Raphson iterative method involving the wave celerity is used to determine these pressure curves. Computed results obtained by this method compare well with the numerical results based upon the characteristics method.

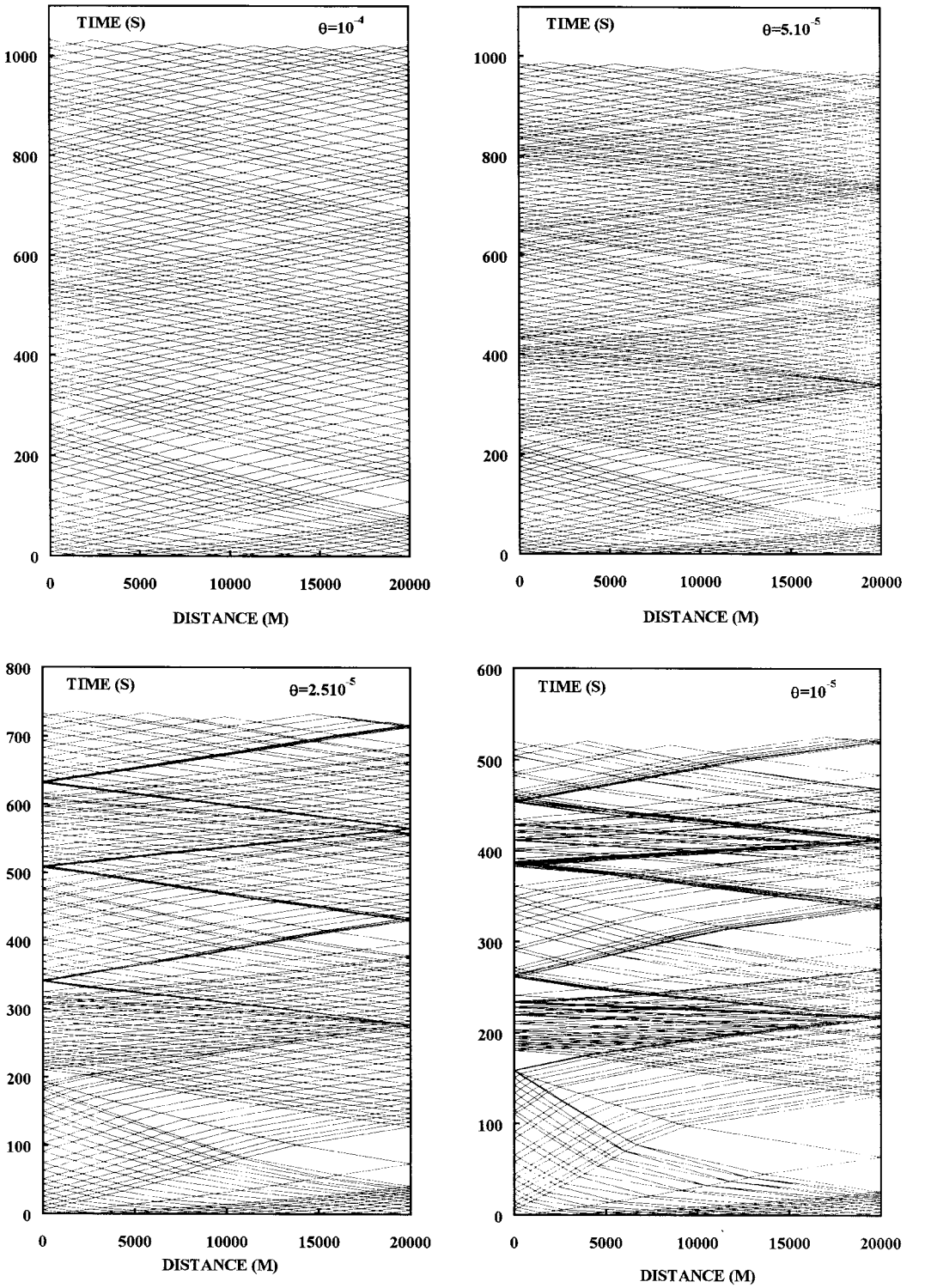

Figure 10. The calculated wave paths for different values of the quality ($N = 20$).

REFERENCES

1. I.J. Campbell and A.S. Pitcher, 'Shock waves in liquid containing gas bubbles', *Proc. Roy. Soc. Lon.*, **243**, 534–545 (1958).
2. C.S. Martin, M. Padmanabhan and D.C. Wiggert, 'Pressure wave propagation in two-phase bubbly air–water mixtures', *2nd Int. Conf. on Pressure Surges*, City University, London, UK, Paper C1, 1976, pp. 1–16.
3. M.H. Chaudry, S.M. Bhallamudi, C.S. Martin and M. Naghash, 'Analysis of transient in bubbly homogeneous, gas–liquid mixtures', *ASME J. Fluids Eng.*, **112**, 225–231 (1990).
4. D.C. Wiggert and M.J. Sundquist, 'The effect of gaseous cavitation on fluid transients', *ASME J. Fluids Eng.*, **101**, 79–86 (1979).
5. H. Pascal, 'Compressibility effect in two-phase flow and its application to flow metering with orifice plate and convergent–divergent nozzle', *Trans. ASME J. Fluids Eng.*, **105**, 394–399 (1983).
6. V.L. Streeter and E.B. Wylie, *Hydraulic Transients*, FEB Press, Ann Arbor, 1982.
7. M.B. Abbott, *An Introduction to the Method of Characteristics*, Elsevier, New York, 1966.
8. S. Stuckenbruck and D.C. Wiggert, 'Unsteady flow through flexible tubing with coupled axial wall motion', *5th Int. Conf. on Pressure Surges*, Hannover, Germany, Sept. 11–17, 1986.
9. F.B.F. Rachid and S. Stuckenbruck, 'Transient in liquid and structure in viscoelastic pipes', *6th Int. Conf. on Pressure Surges*, Cambridge, UK, Paper C2, 1989.
10. A.S. Tijsselmg and C.S.W. Lavooij, 'Fluid-structure interaction and column separation in a straight elastic pipe', *6th Int. Conf. on Pressure Surges*, Cambridge, UK, Paper A2, 1989.
11. P.D. Lax and B. Wendroff, 'Difference schemes for hyperbolic equations with high order of accuracy', *Comm. Pure Appl. Math.*, **17**, 381–398 (1966).
12. A. Lerat and R. Peyret, 'Sur le choix des schémas aux différences du second ordre fournissant des profils de choc sans oscillations', *CR Acad Sc Paris t.*, **277**, (1973).
13. E. Hadj-Taieb and T. Lili, 'Transients in flexible pipes with gas release', *7th Int. Conf. on Pressure Surges and Fluid Transients in Pipelines end Open Channels*, Harrogate, UK, 1996, pp. 109–118.
14. J. Stoer and R. Burlisch, *Introduction to Numerical Analysis*, Springer, Berlin, 1983.
15. T. Strelkoff, 'Numerical solution of Saint-Venant equations', *J. Hydraul. Div. ASCE*, **96**, (HY1), 223–252 (1970).

